

Research Article

Study of the Transient Natural Convection of a Newtonian Fluid inside an Enclosure Delimited by Portions of Cylinders

Omar Ngor Thiam, Samba Dia, Pierre Faye, Cheikh Mbow and Joseph Sarr
Laboratoire De Mecanique Des Fluides Et Applications, Département De Physique, Faculte
Des Sciences Et Techniques Université Cheikh Anta DIOP Dakar-Fann, Senegal

Abstract: Using a bi-cylindrical coordinates system and a vorticity-stream function formulation, the authors study numerically the two dimensional unsteady natural convection of a Newtonian fluid bounded by portions of cylinders. A spatial discretization based on the finite difference method is used to approximate the dimensionless equations. While a purely implicit scheme is adopted for the time discretization. The algebraic systems of equations resulting from the discretization are solved by a Successive under Relaxation (SUR) method. The authors analyzed the effects of the Rayleigh number on the dynamic of the system. The analysis of the thermal and flow field showed that for Rayleigh number greater than 5.10^6 the transfers inside the enclosure are dominated by convection.

Keywords: Bi-cylindrical coordinates, convection, flow, fluid, heat transfer

INTRODUCTION

The study of the natural convection in an enclosure delimited by portions of cylinders provides a better understanding of the heat transfer in various industrial applications such as thermal power station, solar collectors, fluid storage, water industrial heating and the flow in cylindrical shapes warehouse.

In a theoretical and experimental study of natural convection in an annular sector, Sarr *et al.* (2001) observed that the limit of the conductive regime corresponded to a Grash of number equal to 10^3 and they also found that when the shape factor increases the heat transfers are more intense.

Using a finite volume method and equations written in an elliptical coordinates system, (Djezzar and Daguene, 2004) studied the effect of the elliptical shape of the lower cylinder on heat transfer. Roschina *et al.* (2005) studied the natural convection between two horizontal concentric cylinders with energy generation inside; they considered a second thermal Rayleigh number for the transfer through the faces, different from the classical one. For low Rayleigh numbers, they observed two types of flows with different vortex structure.

Shi *et al.* (2006) simulated the transfer of heat by natural convection in a concentric horizontal annular space by finite difference based on lattice Boltzmann method, the flow and thermal field were obtained for Rayleigh numbers between $2.38.10^3$ to $1.02.10^5$ they find that if $Ra < 3.20.10^4$ heat transfer is dominated by the conduction.

In the study of Sankar *et al.* (2011), the study of the natural convection in a vertical ring filled with a saturated porous material, the analysis of a wide range of Rayleigh and Darcy number with various lengths of the heat source reveal source revealed that increasing ratio radius, Rayleigh number and Darcy number, increases heat transfer, while the heat transfer decreases when the length of the heating element increases.

METHODOLOGY

Mathematical approach: The aim of this study is to study the laminar natural convection in an enclosure delimited by no concentric portions of cylinders (Fig. 1). At $t < 0$ the enclosure is at the temperature T_0 from this date, a heat flow of constant density q is abruptly imposes on the cylindrical wall interior θ_1 , the outer wall θ_2 is maintained at a constant temperature T . The other two walls (η_1 and η_2) are thermally insulated ($q = 0$).

To formulate and solve this problem it is assumed that:

- The phenomena are two-dimensional and symmetrical.
- All fluid properties are taken to be constant, with the exception of the density in the momentum equation. In this equation variations of density obey to the Boussinesq linear law.
- The fluid is non absorbing and the radiative effects are regarded as negligible.

Corresponding Author: Omar Ngor Thiam, Laboratoire de Mécanique des Fluides et Applications, Département de Physique, Faculté des Sciences et Techniques Université Cheikh Anta DIOP Dakar-Fann, Sénégal

This work is licensed under a Creative Commons Attribution 4.0 International License (URL: <http://creativecommons.org/licenses/by/4.0/>).

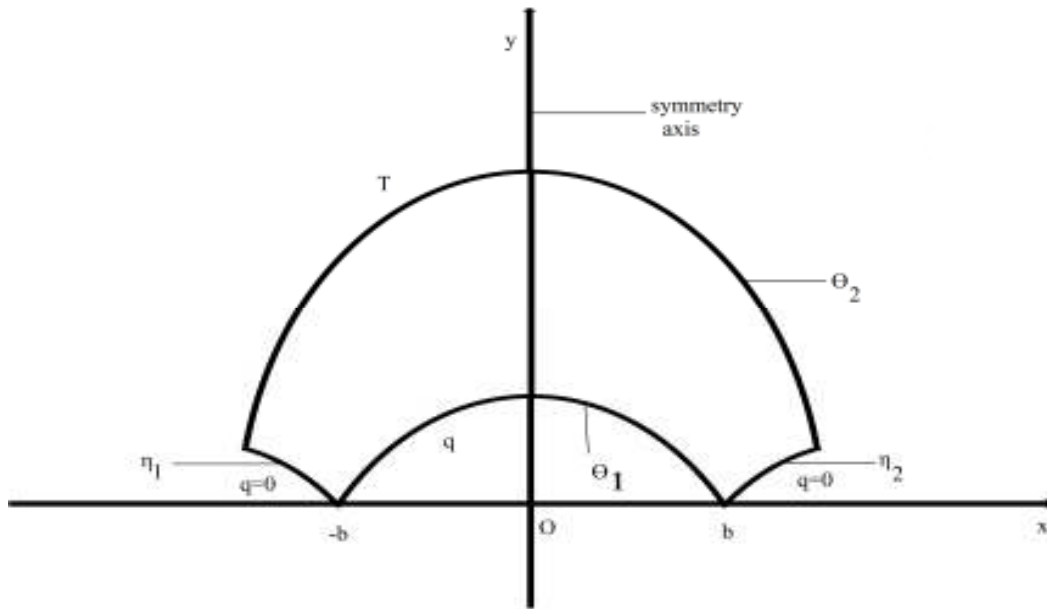


Fig. 1: Geometry of the problem

- In the heat equation the viscous dissipation function as well as the compression effects are neglected.

Taking into account the geometry of our enclosure, we employ a bi-cylindrical coordinate systems (η, θ) (Moon and Spencer, 1971) in which the boundaries of our cavity are given by constant coordinates lines. The passage of Cartesian coordinates to the bi-cylindrical coordinates is carried out using the following relations:

$$x = \frac{b \sinh \eta}{\cosh \eta - \cos \theta}$$

$$y = \frac{b \sin \theta}{\cosh \eta - \cos \theta}$$

$$z = z$$

with b the parameter of torus pole.

From the above assumptions and the coordinate transformation, the governing equations in a dimensionless vorticity-stream function $(\Omega - \psi)$ form are:

Stream function equation:

$$\Omega = -\frac{1}{H^2} \left(\frac{\partial^2 \psi}{\partial \eta^2} + \frac{\partial^2 \psi}{\partial \theta^2} \right) \quad (1)$$

Momentum equation:

$$\frac{\partial \Omega}{\partial t} + \frac{U}{H} \frac{\partial \Omega}{\partial \eta} + \frac{V}{H} \frac{\partial \Omega}{\partial \theta} = \frac{Pr}{H^2} \left[\frac{\partial^2 \Omega}{\partial \eta^2} + \frac{\partial^2 \Omega}{\partial \theta^2} \right] + \frac{Ra^* Pr}{H} \left[G_1 \frac{\partial T}{\partial \eta} + G_2 \frac{\partial T}{\partial \theta} \right] \quad (2)$$

Heat equation:

$$\frac{\partial T}{\partial t} + \frac{U}{H} \frac{\partial T}{\partial \eta} + \frac{V}{H} \frac{\partial T}{\partial \theta} = \frac{1}{H^2} \left[\frac{\partial^2 T}{\partial \eta^2} + \frac{\partial^2 T}{\partial \theta^2} \right] \quad (3)$$

where,

$$U = \frac{1}{H} \frac{\partial \psi}{\partial \eta} \quad (4)$$

$$V = \frac{-1}{H} \frac{\partial \psi}{\partial \theta}$$

The length, velocity, stream function, vorticity and time of reference are respectively define as:

$$b, \frac{\alpha}{b}, \alpha, \frac{\nu}{b^2}, \frac{b^2}{\alpha}$$

And the scale of temperature is $\frac{qb}{\lambda}$.

The associated initial and boundary conditions for the problem considered are:

At $t < 0$

$$U(\eta, \theta) = V(\eta, \theta) = \psi(\eta, \theta) = \Omega(\eta, \theta) = T(\eta, \theta) = 0 \quad (5)$$

At $t > 0$ the boundary conditions are the following ones:

- On the inner cylinder $(\theta = \theta_1)$:

$$U = V = \frac{\partial \psi}{\partial \theta} \Big|_{\theta=\theta_1} = \frac{\partial \psi}{\partial \eta} \Big|_{\theta=\theta_1} = 0 \quad (6)$$

$$\Omega = \frac{-1}{H^2} \frac{\partial^2 \psi}{\partial \theta^2} \Big|_{\theta=\theta_1} \quad (7)$$

$$\left. \frac{\partial T}{\partial \theta} \right|_{\theta=\theta_1} = -H \quad (8)$$

- On the outer cylinder ($\theta = \theta_2$):

$$U = V = \left. \frac{\partial \psi}{\partial \theta} \right|_{\theta=\theta_2} = \left. \frac{\partial \psi}{\partial \eta} \right|_{\theta=\theta_2} = 0 \quad (9)$$

$$\Omega = \left. \frac{-1}{H^2} \frac{\partial^2 \psi}{\partial \theta^2} \right|_{\theta=\theta_2} \quad (10)$$

$$T = 0 \quad (11)$$

- On the wall η_1 and η_2 :

$$U = V = \left. \frac{\partial \psi}{\partial \eta} \right|_{\eta=\eta_1, \eta_2} = \left. \frac{\partial \psi}{\partial \theta} \right|_{\eta=\eta_1, \eta_2} = \left. \frac{\partial T}{\partial \eta} \right|_{\eta=\eta_1, \eta_2} = 0 \quad (12)$$

$$\Omega = \left. \frac{-1}{H^2} \frac{\partial^2 \psi}{\partial \eta^2} \right|_{\eta=\eta_1, \eta_2} \quad (13)$$

- On the symmetry axis ($\eta = 0$):

$$\frac{\partial U}{\partial \eta} = \frac{\partial V}{\partial \eta} = \frac{\partial \psi}{\partial \eta} = \frac{\partial T}{\partial \eta} = \frac{\partial \Omega}{\partial \eta} = 0 \quad (14)$$

The local and the average Nusselt number and friction coefficient relative to the lower cylindrical are defined by:

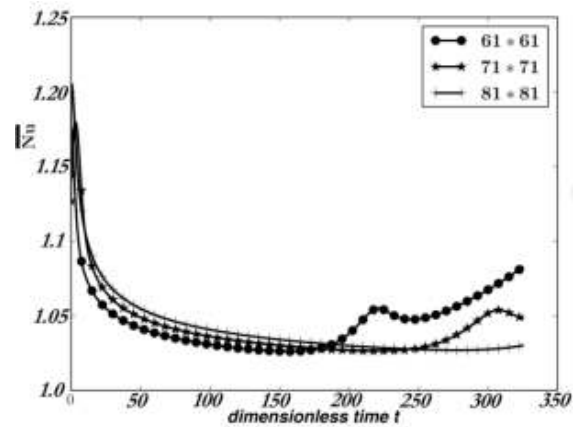
$$Nu = \frac{1}{T - T_p} \quad \overline{Nu} = \frac{1}{S} \int Nu \cdot ds \quad (15)$$

$$Cf = \frac{2 \text{Pr}}{H} \cdot \frac{\partial V}{\partial \theta} \quad \overline{Cf} = \frac{1}{S} \int Cf \cdot ds$$

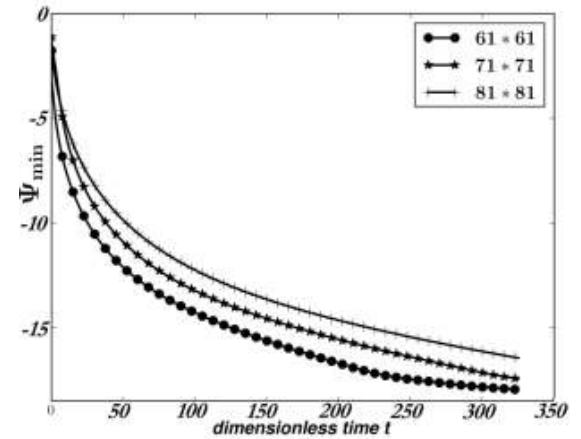
T_p is the dimensionless temperature of the outer cylinder ($\theta = \theta_2$).

Numerical formulation: Equations are integrated numerically using a finite difference method. The spatial discretization is made by a finite difference method. A fully implicit procedure is retaining for treating the temporary derivatives (Bejan, 2004). The resulting algebraic equations were solved by Successive under Relaxation method (SUR) (Patankar, 1980). The iterative process is repeat until there is no significant change of the value F compared to the criterion of convergence:

$$\frac{F^{n+1} - F^n}{F^{n+1}} < \epsilon_r \quad (16)$$



(a)



(b)

Fig. 2: Variation of the nusselt number and the minimal of the stream function against

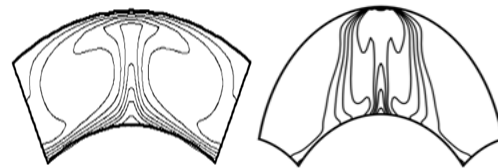


Fig. 3: Isotherms observed for Sarr at $Gr = 0.1 \cdot 10^7$ and for Thiam at $Ra = 10^7$

where, n is the incrementing index of the iterative process and ϵ_r his precision.

The grid size selected is equal to (71*71), with uniform grid spacing in both directions, (Fig. 2) shows the influence of the grid system according to the instantaneous average Nusselt number \overline{Nu} on the inner cylinder ($\theta = \theta_1$) and the minimum value of the stream-function ψ_{min} , the Rayleigh number is fixed at $Ra = 5 \cdot 10^6$. All the results are obtained with $Pr = 0.7$ and a time step $\Delta t = 5 \cdot 10^{-4}$ s retained to carry out all

numerical tests. Refining this time step results in minor changes of the transient patterns.

In order to validate our results, we compare them with those of Sarr *et al.* (2001). In Fig. 3 we can see on the right our isotherms obtained for $Ra = 10^7$ and on the left those observed experimentally by Sarr *et al.* (2001) for a Grashof number $Gr = 0.1 \cdot 10^7$.

Although the geometries and the boundary conditions are not rigorously identical, the topology of the isotherms is quite similar.

RESULTS AND DISCUSSION

Flow fields, temperature fields and heat transfer for various values of the Rayleigh number are examined in this section. The main results are shown in Fig. 4 to 8. These figures show the effects of changing Rayleigh number between 10^6 and 10^7 . Flow and temperature fields are shown respectively in terms of streamlines and isotherms. Owing to the symmetrical boundary conditions, the flows in the left and right of the symmetry axis are identical except for the sense of rotation.

When $Ra < 5 \cdot 10^6$ (Fig. 4) the circulation of the fluid is weak. At the first moments, the isotherms are curves almost parallel with the profile of the enclosure. In this case the distribution of the temperatures is simply decreasing from the hot wall towards the cold wall. The flow consists of a single and large clockwise cell (dotted line). Fluid particles move upwards under the action of the buoyancy along the hot inner cylinder then go down in the vicinity of the cold wall from the external cylinder. With time, the parallelism of the isotherms with the active wall weakens; one observes also the formation of a boundary layer thermal. Indeed, the isotherm lines instead of progressing towards the upper wall are gradually getting closer to the lower wall.

We are in the presence of a pseudo-conductive mode.

For $Ra \geq 5 \cdot 10^6$ (Fig. 5 and 6) we see that the deformation of the isotherms occur at an early stage.

During a long interval of time, the isotherms always have a cylindrical shape and are more and more confined in area close to the active wall. The regime is still pseudo-conductive with always the presence of a boundary layer thermal whose thickness decreases with increasing values of the Rayleigh number. But for $t = 240$ for $Ra = 5 \cdot 10^6$ and $t = 192$ for $Ra = 10^7$, we note a progressive detachment of the isotherms due to the appearance of a trigonometric cell adjacent to the symmetry axis. As this trigonometric cell is developing pushing the clockwise cell towards the η_2 coordinate wall, we observe a very strong distortion of isotherms. We have a convective mode of heat transfer.

However, it is important to note that the thermal and flow field is divided into two distinct parts:

- A zone close to the symmetry axis where the thermal front fills the annular space (related to the trigonometric cell)
- A zone close to wall η (link the clockwise cell) where we observe always the presence of the thermal boundary layer

The Fig. 7 shows us the variation of the average Nusselt number \overline{Nu} on the inner cylinder ($\theta = \theta_1$) according to time for different Raleigh numbers. For $Ra = 10^6$, there is a monotonous decrease of the average Nusselt number. As for $Ra = 5 \cdot 10^6$ and $Ra = 10^7$, there is also a monotonous decrease but the occurrence of trigonometric cell will still lead to an increase in the average Nusselt number.

A rather similar observation can be made in Fig. 8 describing the evolution of the average coefficient of friction \overline{Cf} on the inner cylinder. Indeed, if for the three

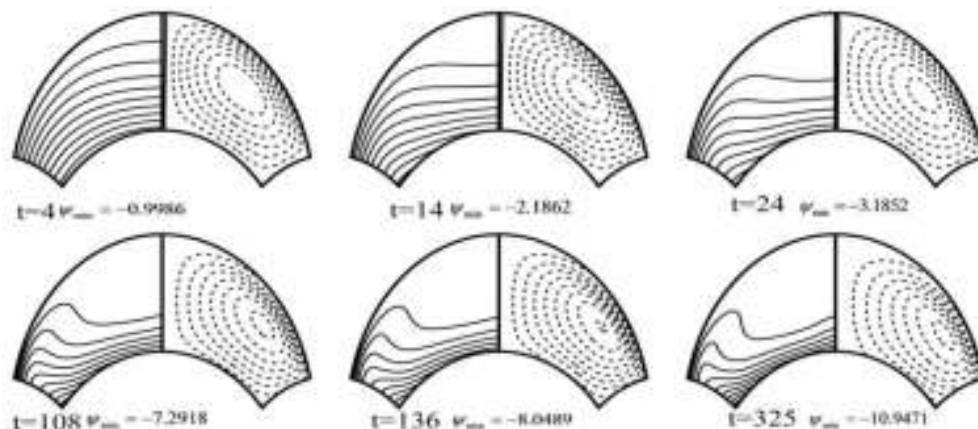


Fig. 4: Evolution of isotherms and streamlines at $Ra = 10^6$

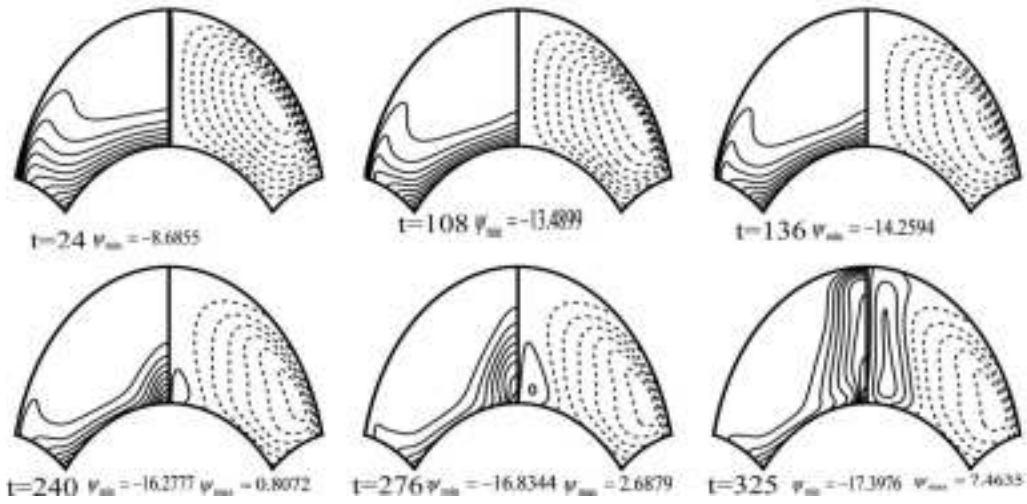


Fig. 5: Evolution of isotherms and streamlines at $Ra = 5.10^6$

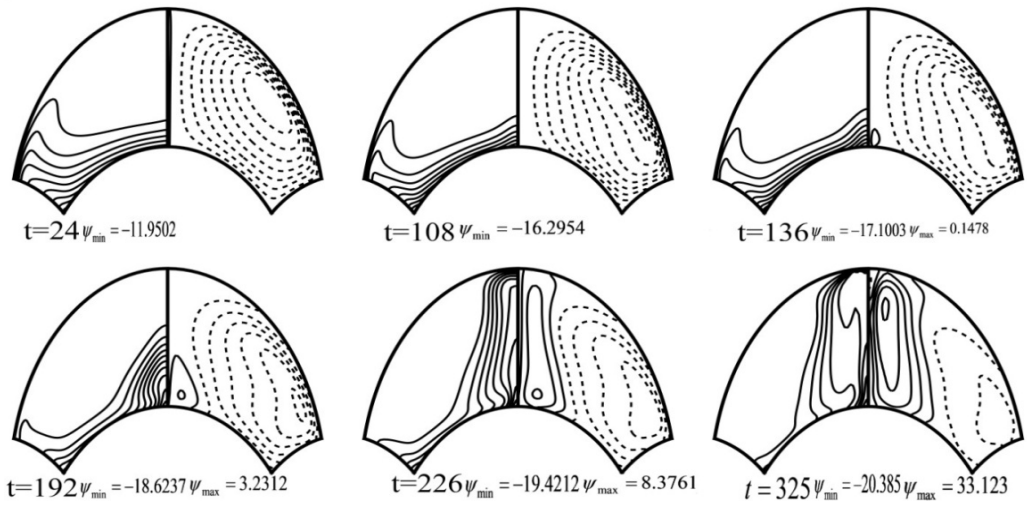


Fig. 6: Evolution of isotherms and streamlines at $Ra = 10^7$

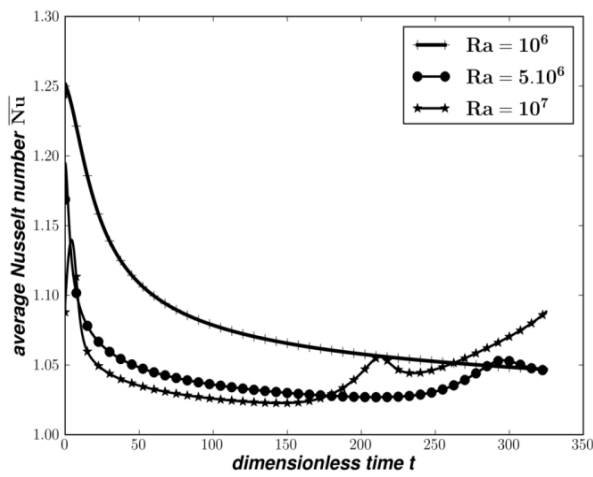


Fig. 7: Variation of the average nusselt number against dimensionless time for various values of Ra

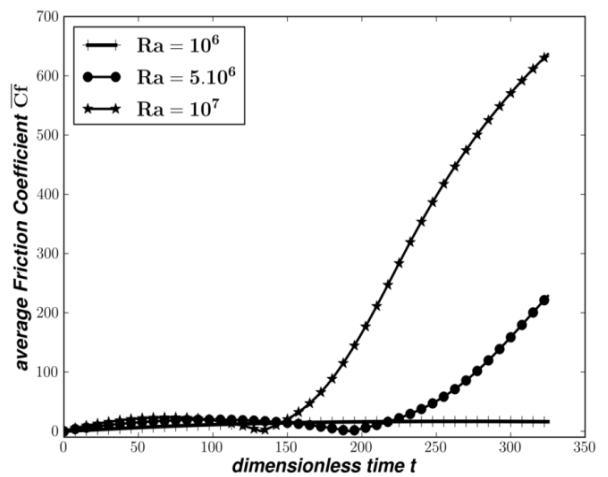


Fig. 8: Variation of the average friction coefficient against dimensionless time for various values of Ra

values of Ra the relatively low values of \overline{Cf} change very little during time, the appearance of the trigonometric cell for the last two values of Ra will lead to a sudden and rapid growth of \overline{Cf} .

CONCLUSION

This study concerns the natural convection in an enclosure delimited by portions of cylinders. The analysis of the dynamic and thermal fields has shown that:

- For $Ra \leq 10^6$, the mode of heat transfer is pseudo-conductive with the formation of a thermal layer. The flow only consists of a clockwise cell occupying all the annular space.
- For $Ra \geq 5.10^6$, throughout the period where the flow is unicellular (clockwise cell) the regime is always pseudo-conductive with the presence of the thermal boundary layer. The convective mode must only be established with the appearance of the trigonometric cell, which leads to a strong development of thermal exchanges in the adjacent zones to the symmetry axis.

NOMENCLATURE

Latin letter:

b	: Parameter of torus pole (m)
C_f	: Friction coefficient
$\overline{C_f}$: Average friction coefficient
F	: Function symbolic system representing the vorticity or the temperature
G_1 and G_2	: Coefficients $G_1 = G_1(\eta, \theta) = \frac{1 - \cos \theta \cosh \eta}{\cosh \eta - \cos \theta}$ and $G_2 = G_2(\eta, \theta) = \frac{-\sin \theta \sinh \eta}{\cosh \eta - \cos \theta}$
H	: Metric coefficients dimensionless $H = \frac{1}{\cosh \eta - \cos \theta}$
h	: Coefficient of transfer of heat by convection $h = \frac{q}{\Delta T} (Wm^2/K)$
Nu	: Nusselt number $Nu = \frac{hb}{\lambda}$
\overline{Nu}	: Average Nusselt number
Pr	: Prandtl number $Pr = \frac{\nu}{\alpha}$
q	: Heat flux density (Wm^2)
Ra	: Rayleigh number $Ra = \frac{g\beta b^4 q}{\nu \alpha \lambda}$
t	: Dimensionless time (s)
T	: Dimensionless temperature (K)

T_0	: Temperature at the initial moment (K)
U, V	: Dimensionless velocity components in the transformed plane
x, y, z	: Cartesian coordinates (m)

Greek symbols:

α	: Thermal diffusivity (m^2/s)
β	: Thermal expansion coefficient (K^{-1})
η, θ, z	: Bicylindrical coordinates (m)
ΔT	: Difference of temperature between the two cylinder activated
Δt	: Time step (s)
λ	: Thermal conductivity (Wm^{-1}/K)
ν	: Kinematical viscosity (m^2/s)

Centre:

Ψ	: Dimensionless stream function
Ω	: Dimensionless vorticity

REFERENCES

- Bejan, A., 2004. Convection Heat Transfer. John Wiley and Sons, New York, pp: 673.
- Djezzar, M. and M. Daguinet, 2004. Numerical study of bidimensional steady natural convection in a space annulus between two elliptic cofocal ducts. Proceeding of 1st International Conference on Thermal Engineering Theory and Applications. Beirut-Lebanon.
- Moon, P. and D. Spencer, 1971. Field Theory Handbook. Springer, Berlin.
- Patankar, S.V, 1980. Numerical Heat Transfer and Fluid Flow. McGraw Hill, New York.
- Roschina, N.A., A.V. Uvarov and A.I. Osipov. 2005. Natural convection in an annulus between coaxial horizontal cylinders with internal heat generation. Int. J. Heat. Mass. Tran., 48: 4518-4525.
- Sankar, M., P. Youngyong, J.M. Lopez and D. Younghae, 2011. Numerical study of natural convection in a vertical porous annulus with discrete heating. Int. J. Heat. Mass. Tran., 54: 1493-1505.
- Sarr, J., M. Sall, M.M. Kane, B. Ba and M. Daguinet, 2001. Numerical natural convection in a sector-shaped enclosure. Int. J. Numer. Method. H., 11(4): 342-357.
- Shi, Y., T.S. Zhao and Z.L. Guo, 2006. Finite difference-based Lattice Boltzmann simulation of natural convection heat transfer in a horizontal concentric annulus. Comput. Fluids, 35: 1-15.